Applied Physics Letters ARTICLE pubs.aip.org/aip/apl

Computationally guided experimental validation of divacancy defect formation in 4H-SiC

Cite as: Appl. Phys. Lett. **126**, 164001 (2025); doi: 10.1063/5.0255575
Submitted: 30 December 2024 · Accepted: 9 April 2025 ·
Published Online: 23 April 2025

Taishi Kimura,[1,2,a] Jonghoon Ahn,[2,3] Nazar Delegan,[2,3,4] Alan Dibos,[3,4] Jiefei Zhang,[2,3,4] Benjamin Pingault,[2,3,4,5] Cunzhi Zhang,[5] Giulia Galli,[2,3,4,5] David Awschalom,[2,3,4,5,6] and F. Joseph Heremans[2,3,4,5,a]

AFFILIATIONS

[1]Toyota Research Institute of North America, 1555 Woodridge Avenue, Ann Arbor, Michigan 48105, USA
[2]Materials Science Division, Argonne National Laboratory, Lemont, Illinois 60439, USA
[3]Center for Molecular Engineering, Argonne National Laboratory, Lemont, Illinois 60439, USA
[4]Q-NEXT, Argonne National Laboratory, Lemont, Illinois 60439, USA
[5]Pritzker School of Molecular Engineering, University of Chicago, Chicago, Illinois 60637, USA
[6]Department of Physics, University of Chicago, Chicago, Illinois 60637, USA

Note: This paper is part of the Special Topic, Defects in Solids for Quantum Technologies.
[a]**Authors to whom correspondence should be addressed:** taishi.kimura2@toyota.com and heremans@anl.gov

ABSTRACT

Recent research into solid-state qubits for quantum information science has focused on optically addressable spin defects such as the negatively charged nitrogen-vacancy center in diamond and the neutrally charged divacancy (VV) in 4H-SiC as scalable quantum sensors and networking qubits. Within this context, direct investigations of the structural origin and defect formation dynamics of a sub-set of the VV center in 4H-SiC remain lacking. Here, we take a systematic experimental approach guided by predictions from first-principles simulations to gain a thorough mechanistic understanding of the VV defect formation and control in 4H-SiC. We study the effect of annealing time and temperature on VV formation in high-purity semi-insulating 4H-SiC samples following electron irradiation. Three different temperatures (1123, 1273, and 1473 K) and annealing duration (from 0.5 to 72 h) are chosen to explore VV formation in different regions. We find that samples annealed at 1273 K give the highest VV-related photoluminescence (PL) intensities, in agreement with the prediction from first-principles calculations. Furthermore, the logarithmic dependence of VV-related PL intensities on the annealing duration at 1273 K indicates that 1273 K provides sufficient thermal energy for silicon vacancy migration but not for VV migration. Together, these results suggest that efficient VV formation occurs above the V_{Si} migration temperature and below the VV migration threshold.

Optically addressable defect spins in the solid state, such as the negatively charged nitrogen-vacancy center in diamond, have been of interest for over a decade for applications in quantum technologies, such as scalable quantum sensing and quantum networking.[1–8] Beyond diamond, a number of interesting and viable host materials and point defect color centers have been reported. As one such example, 4H-SiC hosts a variety of color centers, including the negatively charge state silicon vacancy (V_{Si}),[2,9–12] neutral charge state divacancy (VV),[2,9–11,13–15] transition metal defects (Cr^{4+} and V^{4+}),[16–18] and nitrogen–silicon vacancy pairs (NV).[2,9–11] Among these spin defects, VV in 4H-SiC has emerged a candidate system for quantum information science applications, showing an easily addressable spin-photon manifold with near-infrared emission, long coherence times,[2,9–11,13–15] while hosted in 4H-SiC, a technologically and industrially promising semiconductor material with well-established multi-inch-scale growth, demonstrated device engineering, and well-developed electrical bandgap engineering (n-type and p-type).[19] Despite these advantages, a few key scientific challenges remain. Critically, deterministic synthesis of intrinsic single- and divacancy centers remains difficult due to a lack of quantitative understanding of the underlying formation dynamics. In this context, both proton irradiation and laser annealing were used to better understand the defect formation dynamics.[20–22] However, due to the combination of unexplored thermal regimes, as well as process induced undesirables, a clear and unobstructed picture of the formation dynamics remains elusive.

In this study, we provide an experimentally systematic, molecular dynamics modeling guided approach to elucidate intrinsic defect formation mechanism in 4H-SiC at a broad range of relevant temperatures.[23,24] Our combined research results demonstrate that efficient VV formation should occur above the V_{Si} migration temperature and below the VV migration threshold. Recent modeling and calculations predicted appropriate temperature ranges for the preferential formation of VV in bulk high-purity semi-insulating (HPSI) 4H-SiC to be approximately between 1150 and 1300 K as shown in Fig. 1.[23,24] However, these calculations were carried out based on the cubic crystal of 3 C-SiC, motivating the need to extend these calculations to guide and interpret the defect formation in the hexagonal crystal of 4H-SiC.[23,24] Based on the cubic modeling results, at temperatures below 1150 K, the silicon vacancy (V_{Si}) is less likely to migrate and combine with a carbon vacancy (V_C) to form VV. Whereas at temperatures above 1300 K, VV can migrate easily to the deeper region or surfaces of the sample, resulting in PL intensity decrease due to increased photon absorption or reflection in the deeper region or surface annihilation of VVs. This is the mechanism we observe, by which the VV formation may be primarily limited by V_{Si} migration.[25] Furthermore, our results provide compelling evidence that these simulations are valid beyond just 3 C-SiC, providing a framework for additional simulations in other SiC polytypes. This computationally guided approach could therefore be expanded to formation dynamics studies exploring other types of color centers in SiC.

The host material used in this study is a commercially available high-purity semi-insulating (HPSI) 4H-SiC substrate acquired from STMicroelectronics. The samples were diced to approximately $4 \times 6\,mm^2$ and chemically cleaned with acetone, IPA, and DI water. The samples were then electron irradiated with a beam energy of 2 MeV and fluence $2 \times 10^{16}\,cm^{-2}$ at room temperature. This electron irradiation energy was sufficient for the creation of both C and Si atom displacement with the electron penetration depth exceeding the sample thickness (~300 μm), providing for a uniform V_{Si} and V_C creation profile.[26,27]

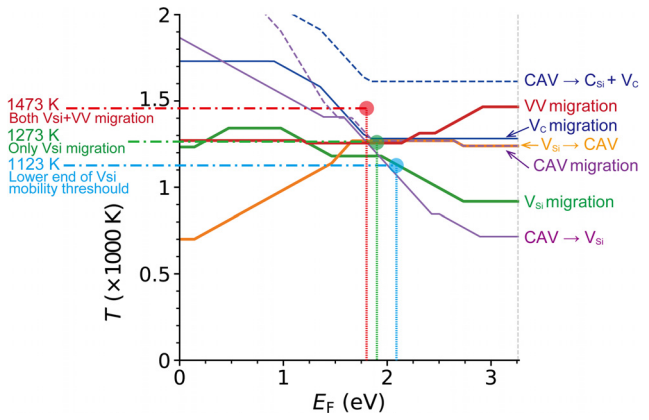

FIG. 1. The original figure came from the theoretical calculation paper of Cunzhi *et al.*[23,24] Computed activation temperature as a function of the Fermi level (E_F).[23,24] The red, green, and blue circles indicate the points are coordinated by the annealing temperatures and calculated Fermi levels used in this study.[23] The blue, green, and red dash-dotted lines represent each annealing temperature, and dotted lines represent the calculated Fermi level at each annealing temperature.

The Fermi level position of the sample is a key variable to ascertain, as the formation energy of each defect depends on the Fermi level position. To confirm the Fermi level position as a function of the donor (N) and acceptor (B and Al) impurity concentrations, the doping concentrations in the HPSI 4H-SiC samples were measured via secondary ion mass spectrometry (SIMS). The average concentration of N, B, and Al in 4H-SiC determined by SIMS was $\sim 3 \times 10^{15}$, $\sim 1 \times 10^{15}$, and $< 1 \times 10^{13}\,cm^{-3}$, respectively (see the supplementary material). The resistivity of this HPSI 4H-SiC wafer was greater than 1×10^{10} ohm-cm, providing a maximum doping concentration mostly of n-type at $1 \times 10^{15}\,cm^{-3}$. From this, we calculate the Fermi level during the high temperature annealing to be ~2.1 eV at 1123 K, 1.9 eV at 1273 K, and 1.8 eV at 1473 K, respectively, as shown in Fig. 1.[23] Of note, Pavel *et al.* reported that electron irradiation introduces acceptor centers such as Z1/Z2 and EH6/EH7 in the 4H-SiC; therefore, the estimated Fermi level may slightly reduce the above-mentioned values due to the compensation of acceptor-like centers.[28]

Figure 1 shows the relationship between the calculated activation temperature of each process and Fermi level. Here, the activation temperature is defined as the temperature above which a process is thermally activated. More details can be found in previous theoretical studies.[23,24] According to Fig. 1, to allow for efficient VV formation (i.e., increase kinetics for VV formation, while minimizing VV diffusion and annihilation), we should choose the highest temperature between the temperature of V_{Si} migration and VV migration, 1123 K is chosen as this threshold. However, 1123 K annealing likely leads to very slow V_{Si} dynamics given that 1123 K is predicted to be on the lower end of V_{Si} mobility threshold. Therefore, a higher temperature is likely ideal in this situation. On the other hand, the 1473 K annealing temperature is high enough to enable the migration of both the V_{Si} and VV; therefore, 1473 K annealing, while allowing for faster V_{Si} diffusion, is also counteracting the desired result due to enabling some VV migration and, as such, annihilation. Therefore, based on these predictions, 1273 K annealing seems to be ideal in this context. From this, three difference annealing temperatures were identified for experimental confirmation, 1123, 1273, and 1473 K. The anneal durations were varied from 0.5 to 72 h to form VV.

To quantify the VV concentrations, we study the PL1—PL4 photoluminescence (PL) spectra. The PL intensity is correlated and proportional to the VV concentrations with all other experimental parameters controlled for as best possible; therefore, we monitor the PL intensity to infer the amount of VV present in the sample.[14,15,29–32] As such, we assumed the formed neutral charge state VV is dominant since the neutral VV state is the most stable in the HPSI or n-type 4H-SiC sample. The non-radiative recombination centers (NRCs) in the samples also could affect the PL intensity. However, we assume the concentration of the NRCs are almost the same among the samples since we employed the same impurity concentration samples and the same dose concentration of electron irradiation. All PL measurements were performed under 905 nm excitation with UV light (centered at 365 nm) illumination to stabilize the bright neutral VV state at 3.9 K using a closed-cycle cryostat (Montana, S50).[15]

Figure 2(a) represents the PL spectra from each sample under different annealing temperatures with a fixed annealing duration of 0.5 h, showing the dependence of V_{Si} or VV diffusion and VV formation on annealing temperature. The PL spectrum of the control sample, as-received, without electron irradiation (EI) and annealing, is also shown

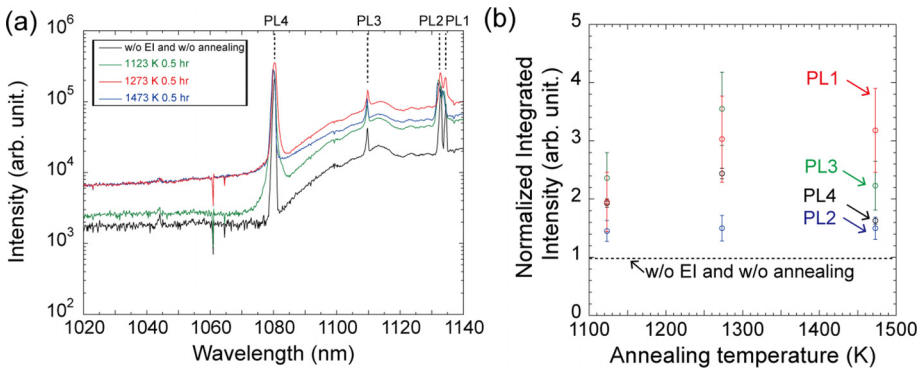

FIG. 2. (a) The photoluminescence spectra of samples with electron irradiation and subsequently annealed at each temperature. The control [without any additional processing except for standard sample cleaning (acetone, IPA, and DI water)] is also shown in this graph. The measurement was carried out at 3.9 K. (b) The normalized integrated PL intensities as a function of annealing temperature. The background correction was carried out for comparison. The error bar represents the 1 σ spread.

in Fig. 2(a). Figure 2(b) shows the normalized integrated PL intensities as a function of annealing temperature. Here, the normalization is carried out using the integrated PL intensity of the control sample (w/o EI and w/o annealing). As shown Fig. 2(b), we observe a universal increase in PL1–PL4 intensities with background subtraction at all annealing temperatures increased compared to the control samples. Critically, the measured PL intensities did not increase when annealing the un-irradiated sample (see the supplementary material). The electron irradiation energy of 2 MeV is high enough to create both V_{Si} and V_C as reported previously.[26,27] Thus, the observed increase in VV in the irradiated samples indicates that both Vsi and Vc are created, and that subsequent annealing is driving the formation of VV within the samples. The background intensity increases were confirmed with increase in the annealing temperature (a similar behavior has been reported by Almutairi *et al.*[21]). These background increases might be caused by vacancy-type defects V_{Si}, VV, or other vacancy-type defects since these defects might have luminescence by broad phonon sideband (PSB) at these wavelength regions. Future work should be verified the origin of the background increase after the annealing.

Higher PL intensity nominally represents a higher VV concentration in this sample, and thus these results corroborate that the annealing temperature of 1123 K is insufficient for mobilizing the V_{Si} and the formation of VV is limited by V_{Si} diffusion. Given the large binding energy between the isolated V_{Si} and V_C in HPSI (or slightly n-type 4H-SiC), VV should be formed once V_{Si} encounters the V_C on its way of diffusion.[23,24]

The normalized integrated intensity of PL1–PL4 for samples annealed at different temperatures is presented in supplementary material, Fig. S3 (see supplementary material). Normalization is carried out using the integrated PL intensity of the control sample with all the processed samples being identical other than their relevant irradiation and annealing processing. It is apparent that each integrated PL1–PL4 intensity is highest when the samples were annealed at 1273 K

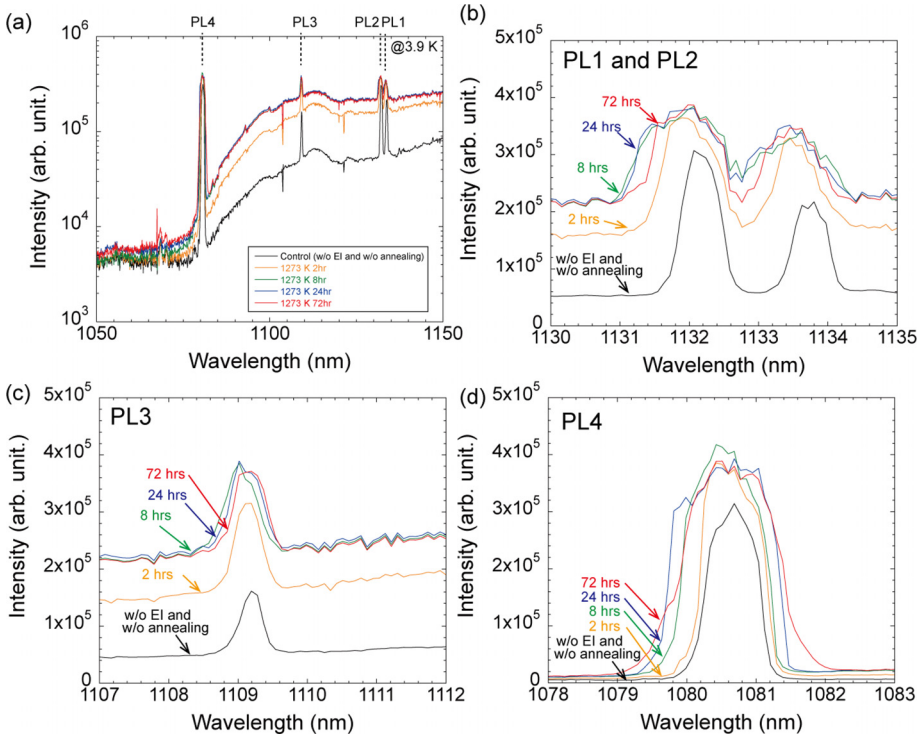

FIG. 3. The PL spectra of samples annealed at 1273 K for 2 h (orange), 8 h (green), 24 h (blue), and 72 h (red) (a), and enlarged PL wavelength area, PL1 and PL2 (b), PL3 (c), and PL4 (d). The PL measurement was carried out at 3.9 K.

compared with those at 1123 and 1473 K. Since the total V_{Si} and V_C concentrations in all samples after electron irradiation should be similar, these observations can be ascribed to the addition of V_{Si} diffusion at higher temperatures in tandem with VV once formed at 1273 K. Furthermore, unlike the samples treated with other annealing temperatures, most of the integrated PL intensities increase with annealing time from 0.5 to 2 h at 1273 K. This increase in PL intensity with annealing time can be explained with the continuous formation of VV where some V_{Si} may need to travel farther within the crystal to aggregate with a V_C. Thus, since the highest increase of PL at 1273 K sample among the samples again confirm that annealing at 1273 K is high enough energy to migrate the V_{Si} and low enough energy to migrate the VV diffusion, consistent with the first-principles simulation results, as shown in Fig. 1.

Conversely, the integrated PL intensity of the sample annealed at 1473 K for 0.5 h does not exceed that of the sample annealed at 1273 K for 0.5 h. Furthermore, most of the integrated PL intensities of the sample annealed at 1473 K for 2 h are almost equivalent (if not slightly decreased) compared with those of the sample annealed at 1473 K for 0.5 h, indicating that VV concentration is stagnated at and above 1473 K. As mentioned above, the temperature of 1473 K should be sufficient to allow migration of V_{Si}, as it is widely understood that V_{Si} is unstable over approximately 800 K and easily forms VV when Vsi encounters Vc.[23,24,31] One possible explanation for the observed reduction of PL intensities is the diffusion of V_{Si} and aggregation with VV to form multi-vacancy, reducing the VV concentration; however, this is not consistent with our results at 1273 K (or other experiments).[20,21] Furthermore, VV should be stable up to 1673 K according to previous results,[31] suggesting VV dissociation is not prevalent. Hence, a reasonable explanation here, we expect, is that VV diffuses into deeper regions or surfaces (annihilated) at longer annealing time. Consequently, the results demonstrate that annealing at 1473 K can provide sufficient thermal energy to mobilize the VVs in the sample. It is evident that our experimental validation results are in good agreement with the first-principles simulation and that these simulations are fully capturing the defect formation dynamics.

Intriguingly, as evident from supplementary material, Fig. S3, the PL intensity trends in all of the conditions indicate that the formation probability of PL1(*hh*), PL2 (*kk*), PL3 (*hk*), and PL4 (*kh*) seems to be different.[32] As shown in supplementary material, Fig. S3, the PL3 (*hk*) intensity is the lowest compared to PL1, PL2, and PL4 intensities. This may suggest that the formation possibility of PL3 (*hk*) is the lowest among PL1–PL4. Bathen *et al.* have reported the formation energy differences among the PL1–PL4 structure as a function of the Fermi level by density functional theory calculation; however, these PL1–PL4 formation energies in the HPSI are almost equivalent.[33] Furthermore, the probability of creating each VV structure may depend not only on the formation energy but also on formation kinetics. Therefore, future work could focus on the formation energy and formation kinetics during annealing and clarify the differences in VV formation and dynamics efficiency for each configuration.

To further verify the existence of VSi diffusion and absence of VV diffusion during annealing at 1273 K, we carried out the longer duration annealing at 1273 K. Figure 3(a) represents the PL spectra obtained from samples after 2–72 h of annealing and enlarged graph of each PL (c–d). Each PL Zero phonon line (ZPL) intensity and background level increases with annealing duration, reaching saturation at around 8 h, and remains almost constant from 8 to 72 h. However, for signal with wavelengths below 1080 nm (close to ZPL of PL4), the background increase is considerably low compared with longer around 1080 nm wavelength region. This hints at the fact that the background level in this spectral regime is associated with the PSB of PL4. Additionally, the peak positions of all ZPLs of PL1–4 are slightly (approximately 0.5 nm) shifted to shorter wavelengths. This can be assumed to arise from compressive local strain in the 4H-SiC crystal lattice due to Vsi diffusion and subsequent divacancy formation during annealing. The maximum shifted energy of PL is approximately 0.5 meV; therefore, the local biaxial stress is roughly estimated at approximately 23 MPa.[34,35]

The dependence of normalized integrated intensity from PL1 to PL4 on annealing duration is shown in Fig. 4, where normalized integrated PL3 (basal) and PL4 (basal) intensities increase significantly from 0.5 to 8 h and reach a steady-state maximum around ~24 h.

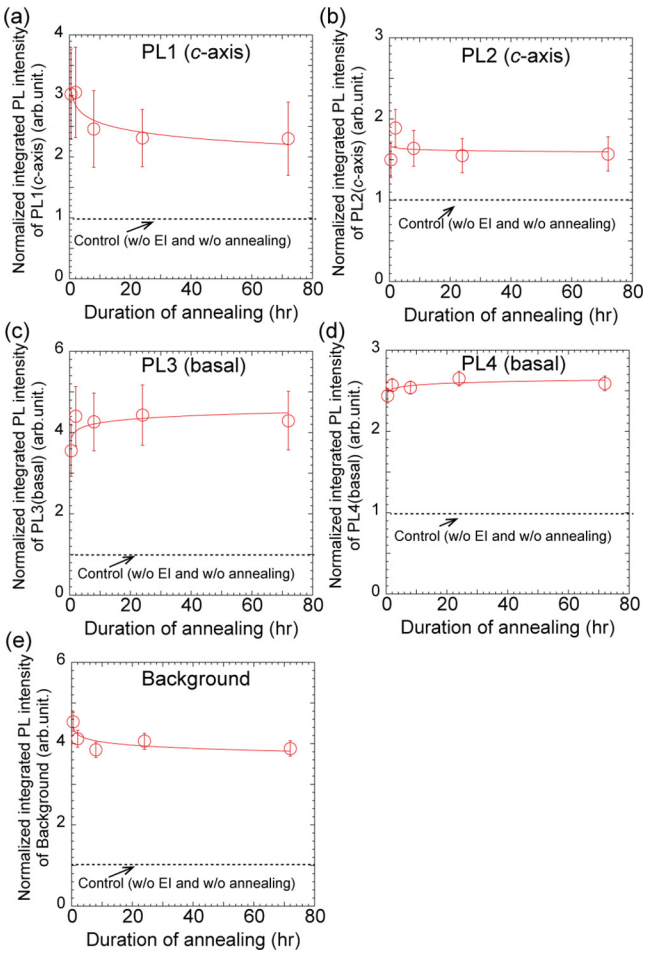

FIG. 4. The normalized integrated PL and background [PL1 (a), PL2 (b), PL3 (c), PL4 (d), and background (e)] intensities as a function of annealing duration at 1273 K. All PL1–PL4 and background intensities were normalized by PL1–PL4 and background values obtained for the control sample (without any process except for cleaning) after background correction. The crystallographic orientation of VV either along the c-axis (PL1-2) or in the basal plane (PL3-4) is indicated. The lines are guides to the eye.

Conversely, the normalized integrated PL1 (*c*-axis) and PL2 (*c*-axis) intensities increase significantly from 0.5 to 2 h and then slightly decrease and reach a steady state around ∼24 h. In addition, the background intensities monotonically decrease with an increased annealing time duration. The maximum normalized integrated PLs in the sample with 2 h of annealing are about 1.9–4.4 times higher compared to those of the control (w/o EI and w/o annealing) sample. As such, our results provide compelling evidence of the feasibility of efficient VV formation by using electron irradiation and subsequent annealing at 1273 K. Therefore, we could surmise that the VV formation is limited by V_{Si} diffusion. Furthermore, once the PL intensities from the VV reached stable values, the PL intensities were almost constant, even after longer durations of annealing. Therefore, these VV may not diffuse to the deeper or surface (annihilated) region at 1273 K annealing, unlike that observed at 1473 K annealing. Consequently, as predicted in the first-principles simulation, 1273 K annealing is best suited for efficient VV formation where V_{Si} can diffuse readily while VV is mostly immobile.

Intriguingly, the integrated PL intensity of c-axis oriented VV (PL1 and PL2) is constant or decreased slightly for 8 h or longer annealing duration. On the other hand, the integrated PL intensity of basal plane oriented VV (PL3 and PL4) increases slightly or constantly for 8 h or longer annealing duration. It might be caused by the crystallographic exchange of VV from c-axis oriented to basal plane oriented VV since the calculated formation energy of each VV is almost equal. Therefore, future studies should verify the formation dynamics of VV during EI and subsequent annealing.

In conclusion, we demonstrate a systematic set of experiments to investigate the formation of VV in 4H-SiC with electron irradiation to generate intrinsic defects and subsequent annealing to mobilize them. Additionally, we validate the proposed formation mechanisms obtained by first-principles simulations.[23,24] As predicted, our results indicate that 1273 K annealing is appropriate for efficient VV formation as the temperature promotes V_{Si} diffusion without VV migration. Our approach used in this study was to combine both theoretical and experimental studies, to better understand the formation mechanism of VV in 4H-SiC, and to clarify and analyze the formation mechanism of the other color centers. Hence, our study provides a framework for future studies to efficiently create ensembles of color centers for future quantum applications and technologies.

See the supplementary material for SIMS analysis results and the comparison of the PL spectra after annealing at 1273 K for 2 h with and without electron irradiation.

This work is primarily funded via CRADA with Toyota Research Institute of North America (T.K. and F.J.H.) in close collaboration with the Materials Science Division supported by the U.S. Department of Energy, Office of Science; Basic Energy Sciences (BES), Materials Sciences, and Engineering (MSE) Division (J.A., N. D., B.P., J. Z., and D.D.A.). The simulation carried out in the study was supported by the Midwest Integrated Center for Computational Materials (MICCoM) as part of the Computational Materials Sciences Program funded by the U.S. Department of Energy, BES, MSE (C.Z., G.G.). The authors acknowledge additional support from the Q-NEXT Quantum Center, a U.S. Department of Energy, Office of Science, National Quantum Information Science Research Center (A.D.). Work performed at the Center for Nanoscale Materials, a U.S. Department of Energy Office of Science User Facility, was supported by the U.S. DOE, Office of Basic Energy Sciences, Contract (No. DE-AC02-06CH11357). The authors thank Dr. Katherine J. Harmon for fruitful discussions.

AUTHOR DECLARATIONS

Conflict of Interest

The authors have no conflicts to disclose.

Author Contributions

Taishi Kimura: Conceptualization (equal); Data curation (equal); Formal analysis (equal); Investigation (equal); Methodology (equal); Project administration (equal); Resources (equal); Validation (equal); Writing – original draft (equal); Writing – review & editing (equal). **Jonghoon Ahn:** Data curation (equal); Formal analysis (equal); Investigation (equal); Validation (equal); Writing – review & editing (equal). **Nazar Delegan:** Data curation (equal); Formal analysis (equal); Investigation (equal); Validation (equal); Writing – review & editing (equal). **Alan Dibos:** Data curation (equal); Formal analysis (equal); Investigation (equal); Validation (equal); Writing – review & editing (equal). **Jiefei Zhang:** Formal analysis (equal); Investigation (equal); Validation (equal); Writing – review & editing (equal). **Benjamin Pingault:** Data curation (equal); Formal analysis (equal); Investigation (equal); Validation (equal); Writing – review & editing (equal). **Cunzhi Zhang:** Investigation (equal); Validation (equal); Writing – review & editing (equal). **Giulia Galli:** Conceptualization (equal); Investigation (equal); Project administration (equal); Validation (equal); Writing – review & editing (equal). **David Awschalom:** Conceptualization (equal); Investigation (equal); Validation (equal); Writing – review & editing (equal). **F. Joseph Heremans:** Conceptualization (equal); Formal analysis (equal); Investigation (equal); Methodology (equal); Project administration (equal); Resources (equal); Writing – review & editing (equal).

DATA AVAILABILITY

The data that support the findings of this study are available within the article and its supplementary material.

REFERENCES

[1]A. Gruber, A. Drabenstedt, C. Tietz, L. Fleury, J. Wrachtrup, and C. vonBorczyskowski, Science **276**(5321), 2012 (1997).
[2]G. Wolfowicz, F. J. Heremans, C. P. Anderson, S. Kanai, H. Seo, A. Gali, G. Galli, and D. D. Awschalom, Nat. Rev. Mater. **6**, 906 (2021).
[3]J. F. Barry, J. M. Schloss, E. Bauch, M. J. Turner, C. A. Hart, L. M. Pham, and R. L. Walsworth, Rev. Mod. Phys. **92**(1), 015004 (2020).
[4]F. J. Heremans, C. G. Yale, and D. D. Awschalom, Proc. IEEE **104**(10), 2009 (2016).
[5]M. W. Doherty, N. B. Manson, P. Delaney, F. Jelezko, J. Wrachtrup, and L. C. Hollenberg, Phys. Rep. **528**, 1–45 (2013).
[6]F. Casola, T. van der Sar, and A. Yacoby, Nat. Rev. Mater. **3**(1), 1–13 (2018).
[7]W. G. Carlo Bradac, J. Forneris, M. E. Trusheim, and I. Aharonovich, Nat. Commun. **10**, 5625 (2019).
[8]S. Esmaeili, P. Schmalenberg, S. T. Wu, Y. Q. Zhou, S. Rodrigues, N. Hussain, T. Kimura, Y. Tadokoro, S. Higashi, D. Banerjee, and E. M. Dede, APL Mater. **12**(4), 040901 (2024).
[9]N. T. Son, C. P. Anderson, A. Bourassa, K. C. Miao, C. Babin, M. Widmann, M. Niethammer, J. Ul Hassan, N. Morioka, I. G. Ivanov, F. Kaiser, J. Wrachtrup, and D. D. Awschalom, Appl. Phys. Lett. **116**(19), 190501 (2020).

[10]A. Lohrmann, B. C. Johnson, J. C. McCallum, and S. Castelletto, Rep. Prog. Phys. **80**(3), 034502 (2017).
[11]B. Magnusson, N. T. Son, A. Csóré, A. Gällström, T. Ohshima, A. Gali, and I. G. Ivanov, Phys. Rev. B **98**(19), 195202 (2018).
[12]R. Nagy, M. Niethammer, M. Widmann, Y. C. Chen, P. Udvarhelyi, C. Bonato, J. U. Hassan, R. Karhu, I. G. Ivanov, N. T. Son, J. R. Maze, T. Ohshima, O. O. Soykal, A. Gali, S. Y. Lee, F. Kaiser, and J. Wrachtrup, Nat. Commun. **10**(1), 1954 (2019).
[13]N. T. Son, D. Shafizadeh, T. Ohshima, and I. G. Ivanov, J. Appl. Phys. **132**(2), 025703 (2022).
[14]W. F. Koehl, B. B. Buckley, F. J. Heremans, G. Calusine, and D. D. Awschalom, Nature **479**(7371), 84 (2011).
[15]G. Wolfowicz, C. P. Anderson, A. L. Yeats, S. J. Whiteley, J. Niklas, O. G. Poluektov, F. J. Heremans, and D. D. Awschalom, Nat. Commun. **8**(1), 1876 (2017).
[16]S. J. W. Berk Diler, C. P. Anderson, G. Wolfowicz, M. E. Wesson, E. S. Bielejec, F. J. Heremans, and D. D. Awschalom npj, Quantum Inf. **6**, 11 (2020).
[17]G. Wolfowicz, C. P. Anderson, B. Diler, O. G. Poluektov, F. J. Heremans, and D. D. Awschalom, Sci. Adv. **6**(18), eaaz1192 (2020).
[18]J. Ahn, C. Wicker, N. Bitner, M. T. Solomon, B. Tissot, G. Burkard, A. M. Dibos, J. Zhang, F. J. Heremans, and D. D. Awschalom, Phys. Rev. Appl. **22**(4), 044078 (2024).
[19]T. Kimoto and H. Watanabe, Appl. Phys. Express **13**(12), 120101 (2020).
[20]R. Karsthof, M. E. Bathen, A. Galeckas, and L. Vines, Phys. Rev. B **102**(18), 184111 (2020).
[21]A. F. M. Almutairi, J. G. Partridge, C. L. Xu, I. S. Cole, and A. S. Holland, Appl. Phys. Lett. **120**(1), 014003 (2022).
[22]H. J. von Bardeleben and J. L. Cantin, Nucl. Instrum. Methods Phys. Res., Sect. B **186**, 201 (2002).
[23]C. Zhang, F. Gygi, and G. Galli, Nat Commun. **14**(1), 5985 (2023).
[24]C. Zhang, F. Gygi, and G. Galli, Phys. Rev. Appl. **8**, 046201 (2024).
[25]E. M. Y. Lee, A. Yu, J. J. de Pablo, and G. Galli, Nat. Commun. **12**(1), 6325 (2021).
[26]H. J. von Bardeleben, J. L. Cantin, L. Henry, and M. F. Barthe, Phys. Rev. B **62**(16), 10841 (2000).
[27]L. Storasta, J. P. Bergman, E. Janzén, A. Henry, and J. Lu, J. Appl. Phys. **96**(9), 4909 (2004).
[28]P. V. Hazdra and J. Phys, Status Solidi A **216**, 1900312 (2019).
[29]A. L. Falk, B. B. Buckley, G. Calusine, W. F. Koehl, V. V. Dobrovitski, A. Politi, C. A. Zorman, P. X. Feng, and D. D. Awschalom, Nat. Commun. **4**, 1819 (2013).
[30]W. E. Carlos, E. R. Glaser, and B. V. Shanabrook, Phys. B **340**, 151 (2003).
[31]W. E. Carlos, N. Y. Garces, E. R. Glaser, and M. A. Fanton, Phys. Rev. B **74**(23), 235201 (2006).
[32]D. A. Golter and C. W. Lai, Sci. Rep. **7**(1), 13406 (2017).
[33]M. E. Bathen, G. M. Selnesaunet, M. J. Enga, S. B. Kjeldby, J. Müting, L. Vines, and U. Grossner, Defect Diffus. Forum **425**, 35 (2023).
[34]H. Y. W. Fu, T. Sakurai, and A. Ueda, Appl. Phys. Express **16**, 081002 (2023).
[35]Z. C. Z. Ni, G. Chen, L. Xueyu, G. Chen, and M. Liu, Appl. Phys. A **131**, 206 (2025).